JOURNAL OF PHYSIOLOGY AND PHARMACOLOGY 2015, 66, 3, 355-366
www.jpp.krakow.pl

E. HUET[1,2], E. GABISON[3], B. VALLEE[1], N. MOUGENOT[4], G. LINGUET[1],
B. RIOU[5], C. JAROSZ[1], S. MENASHI[1], S. BESSE[1,6]

DELETION OF EXTRACELLULAR MATRIX METALLOPROTEINASE INDUCER/CD147 INDUCES ALTERED CARDIAC EXTRACELLULAR MATRIX REMODELING IN AGING MICE

[1]Paris-Est University, Laboratory "Croissance Cellulaire, Reparation and Regeneration Tissulaire", CNRS, Creteil, France; [2]Paris-Est University, INSERM Unit 955, Team 7, Faculty of Medicine, Creteil, France; [3]Paris Diderot University, Sorbonne Paris Cite, and A. de Rothschild Fondation, Paris, France; [4]Pierre and Marie Curie University, Sorbonne Universites, UMS 28 "Phenotypage du petit animal", Faculty of Medicine, Paris, France; [5]Pierre and Marie Curie University, Sorbonne Universites, INSERM UMR 1166 and Department of Emergency Medicine and Surgery, Pitie-Salpetriere Hospital, Assistance Publique-Hopitaux de Paris, Paris, France; [6]Paris-Saclay University, Unit "Biologie Integrative des Adaptations à l'Exercice", INSERM Unit 902, Evry, and Paris-Descartes University, Sorbonne Paris Cite, Paris, France

Extracellular matrix metalloproteinase inducer (EMMPRIN), known for its ability to induce matrix metalloproteinase (MMP) expression, was proposed to play a role in the adverse cardiac extracellular matrix remodeling. After observing an age-associated increase in cardiac EMMPRIN expression in both mice and rats, the role and mechanism of action of EMMPRIN was investigated in the myocardial age-associated changes using 3, 12 and 24 month old EMMPRIN knock-out (KO) vs. wild-type (WT) mice, by cardiac echocardiography, Western blots, immunohistochemistry, ELISA and histology. A dilated cardiomyopathy characterized by a decreased ejection fraction and an enlargement of left ventricular chamber (LV) associated with LV hypertrophy, occurred in KO mice as soon as 12 month old. The increase in interstitial collagen deposition during aging in WT mice could not be detected in KO mice. This may be related to the reduced activation (48% reduction; $P < 0.05$) and signaling (smad2/3 nuclear translocation) of TGF-β in the 12 month old KO mice which paralleled with a greater reduction in the TGF-β known activating enzymes such as MT1-MMP and MMP-1 (33% and 37% reduction respectively, between 3 and 12 month old in KO mice; $P < 0.05$) as well as uPA. These findings demonstrate that EMMPRIN gene silencing is associated with an aberrant extracellular matrix remodeling, characterized by the absence of a detected age-associated fibrosis and consequently to dilated cardiopathy, indicating that a fine regulation of EMMPRIN is essential for the coordinated ECM remodeling during aging.

Key words: *extracellular matrix metalloproteinase inducer, heart, collagen, aging, transforming growth factor-β, smad2-3, membrane type-1-matrix metalloproteinase, fibroblasts, left ventricular hypertrophy*

INTRODUCTION

In the heart, an intricate lattice of collagen-containing extracellular matrix (ECM) surrounds individual myocytes and myofibril bundles, ensuring correct tissue geometry and aiding efficient vectorial transmission of force. The ECM is a dynamic structure and its continuous turnover is under fine control. In the heart, the accumulation of collagen during aging as well as in ischemic or chronic hypertensive cardiopathies, resulting from maladaptative remodeling of cardiac ECM, is believed to increase ventricular stiffness and reduce compliance leading to heart failure (1, 2). By contrast, in congestive cardiopathies, interstitial collagen content is reduced and/or collagen distribution is fragmented, leading to heart failure with cardiac dilation (3).

Matrix metalloproteinases (MMPs), as well as serine proteinases such as uPA, are proteolytic degrading enzymes which cleave extracellular matrix components including collagens, but also activate transforming growth factor-β (TGF-β) which is able to induce collagen I expression in cardiac tissue. A large number of MMPs are expressed within the myocardium but MT1-MMP has been described as particularly involved in the development and progression of myocardial ECM remodeling and consequently heart failure (4, 5). MT1-MMP presents a collagenolytic activity on type I, II, and III collagens and is capable of activating proMMP-2 (6). The extracellular MMP inducer or EMMPRIN (also known as Basigin, or CD147) plays a key regulatory role in MMP synthesis (7). It was first identified as a transmembrane protein on the surface of tumor cells and was shown to stimulate adjacent fibroblasts, endothelial cells or tumor cells to produce MMPs, facilitating the invasion of cancer cells (8). More recently, studies demonstrated the expression of EMMPRIN in cardiac myocytes. Moreover, persistent cardiac-restricted EMMPRIN expression in

mice during aging was associated with increased levels of MT1-MMP, fibrosis, and impaired both left ventricular (LV) geometry and structure, leading to adverse LV remodeling (9). Finally, increased myocardial levels of EMMPRIN, associated with major MT1-MMP induction, have been reported in patients suffering from heart failure.

In this study, we report on EMMPRIN levels in mouse and rat myocardium during aging, especially at the advanced ages in which the development of heart failure was previously demonstrated (10, 11), and on the biological, histological and physiological consequences of a selective disruption of the EMMPRIN gene on myocardial age-associated changes in knock-out (KO) mice, compared to wild type (WT) mice.

MATERIALS AND METHODS

Animals

Three, 12 and 24 month old female WT (n = 6, n = 3 and n = 4, respectively) and EMMPRIN KO (n = 6, n = 5 and n = 3, respectively) C57Bl6 mice (kind gift from T. Muramatsu (12)) and 3, 24, 28 and 32 month old male Wistar rats (n = 6, n = 7, n = 6 and n = 7, respectively) from Charles River Laboratories (L'Arbresle, France) were used. We have chosen to use female rather than male mice to avoid infighting between aggressive male mice. The rate of spontaneous survival is similar between WT (97%, 82% and 62% in 3, 12 and 24 month old, respectively) and EMMPRIN KO (93%, 75% and 58% in 3, 12 and 24 month old, respectively) female mice at all ages. Being infertile, EMMPRIN KO mice were obtained by heterozygous breeding and tail snips were collected for genotyping. DNA was extracted from the snips using DNeasy Blood and Tissue Kit (Qiagen, France) and the genotype was determined by PCR using primers for EMMPRIN and neomycin resistance genes).

All animals were allowed free access to a standard diet and water, maintained at a constant temperature of 22°C and exposed to a 12:12 light-dark cycle.

All *in vivo* experiments were approved by the appropriate French committee in charge of animal experimentation (DDPP, Val de Marne, France) and conducted in compliance with both the international laws and policies (European Communities Council Directive of 24 November 1986, 86/609/EEC) and the Guide for the Care and Use of Laboratory Animals published by the US National Institutes of Health Animal care.

Echocardiography and tissue collection

Transthoracic echocardiography was performed using an echocardiography Doppler VIVID 7 Dimension/Vivid 7 Pro machine (General Electric Medical Systems Co, GE Healthcare, Wauwatosa, WI) with Vivid 7 11-MHz linear probe in 3, 12 and 24 month old WT and EMMPRIN KO mice. Mice were slightly anesthetized with 0.5% isoflurane (Forene®, Abbott, Rungis, France) in oxygen. Modified parasternal long-axis electrocardiogram kilohertz-based visualization loops were also used to measure LV ejection fraction *via* Simpson's method. M-mode recordings in a modified short axis view were used to measure LV chamber sizes and wall thicknesses. LV diameters in diastole and in systole were measured from the mean of at least three separate cardiac cycles.

Hearts from rats and mice were excised after anesthesia (Nesdonal®, 50 mg/kg, Merial, Lyon, France), rinsed in saline solution and blotted and then weighted. Left ventricles were frozen in liquid nitrogen for protein extraction or included in Tissue-Tek O.C.T. Compound (Sakura Finetek, Torrance, CA) for immunohistochemistry.

Western blot analysis

Left ventricles were homogeneized in RIPA buffer (Tris 25 mM, pH = 7.6, NaCl 150 mM, NP-40 1%, sodium deoxycholate 1%) on ice, centrifugated at 13,000 *g* for 15 min at 4°C, and protein quantification was performed in supernatant. Twenty µg of proteins were analyzed by Laemmli SDS-PAGE (Bio-Rad, Marne la Coquette, France) on 10% gels and then transferred to Immobilon-P PVDF membrane (Millipore, Guyancourt, France). Membranes were immunoblotted with anti-EMMPRIN antibody (sc-9757, Santa Cruz Biotechnology, Santa Cruz, CA) overnight at 4°C, or with anti-glyceraldehyde 3-phosphate dehydrogenase (GAPDH) antibody (sc-32233, Santa Cruz Biotechnology) for 1 hour at room temperature, followed by 1 hour incubation with horseradish peroxidase-conjugated anti-mouse secondary antibody (1/10000, Jackson ImmunoResearch, United Kindom) and visualized with chemiluminescent reagent (chemoluminescent Detection System Kit; Chemicon International Inc., Temecula, CA). Protein loading was verified both by ponceau red staining and by comparing with the intensity of GAPDH bands.

Collagen quantification and histomorphometry

LV sections (8 µm) were stained with picro-sirius red to detect collagen fibers and with Masson's trichrome to observe myocyte loss and accumulation of collagen and extracellular matrix. Digital images of sirius red and Masson's trichrome stained sections were acquired using an Olympus microscope (IX81, Olympus, Rungis, France). Quantitative mesurements of LV collagen (12 images at different LV levels per heart) were processed in Sirius red stained sections by a computerized image analyzer (MetaMorph 7.0, Molecular Devices, Saint-Gregoire, France).

Immunohistochemistry

Cryostat sections (8 µm) were prepared from frozen hearts and were immunostained as previously described (10). Briefly, the sections were fixed in chilled acetone for 10 min, then rehydrated in PBS and incubated in blocking solution (5% BSA in PBS) for 45 min.

Sections were incubated for 1 hour with either anti-EMMPRIN (sc-9757, Santa Cruz Biotechnology), anti-pan cadherin (4068, Cell Signaling, Ozyme), anti-zonula occludens-1 (ZO-1; sc-10804, Santa Cruz Biotechnology), anti-connexin 43 (Cnx-43; 3512, Cell Signaling), anti-MMP-1 (IM35L, Merck Millipore), anti-MMP-2 (ab 7032, abcam), anti-MMP-9 (ab38898, abcam), anti-MT1-MMP (IM39, Merck Millipore), anti-fibroblast (M0877, Dako) or anti-smad2/3 (07-408, Merck Millipore) antibodies and then for 1h with conjugated affinity-purified donkey anti-mouse IgG, anti-rabbit or anti-goat IgG Alexa Fluor® 594 or 488 (Life Technologies) antibodies. Digital images of MMP immunolabeled sections were acquired using a confocal Olympus microscope (IX81). Quantitative measurements of immunolabeled protein content (12 images at different LV levels per heart) were processed by a computerized image analyzer (MetaMorph 7.0).

Enzyme-linked immunosorbent assays (ELISA)

Latent and activated TGF-β protein was quantified using the commercial Quantikine TGF-β1 ELISA Kit (R & D Systems, Minneapolis, MN) according to the manufacturer's instructions. Briefly, the tissue extracts were activated with 1 N HCl for 10 min, followed by neutralization with 1.2 N NaOH. The activated samples were applied to the plate precoated with soluble type II receptor and incubated at room temperature for 2 hours. After

extensive washing, horseradish peroxidase-conjugated anti-TGF-β antibody was added and incubated for another 2 hours. Then the chromogen was added, and the plate was read at 450 nm. MMP-1 protein was quantified using the commercial Mouse Matrix Metalloproteinase 1 ELISA Kit from Cusabio® (CliniSciences, Nanterre, France), according to the manufacturer's instructions. All the ELISA results were expressed as picograms per milligram of total protein.

Zymography assay

Activity of urokinase plasminogen activator (uPA) was determined by casein zymography and quantification was processed by computerized densitometry (MetaMorph 7.0). Left ventricular proteins were extracted in RIPA buffer and 20 µg of proteins were separated on 10% SDS-PAGE gels containing 2 mg/mL casein (Sigma-Aldrich, Saint-Quentin Fallavier, France) and 10 µg/mL plasminogen (Calbiochem, Millipore), under non-reducing conditions. Then, the gels were washed twice in 2.5% Triton-X 100 for 30 min, incubated with reaction buffer (50 mM Tris, 150 mM NaCl and 5 mM $CaCl_2$, pH=7.5) for 24 hours at 37°C, and stained with Coomassie blue G-250. Conditioned media of HT-1080, which have the highest baseline uPA activities, were used as a positive control in casein-plasminogen zymography.

Statistical analysis

Data were expressed as mean ± S.E.M. The Gaussian distribution of the data was verified and then statistical analyses were performed using one-way analysis of variance, followed by the Newman-Keuls post hoc test. All P values were two-tailed and $P < 0.05$ was considered as statistically significant.

RESULTS

Extracellular matrix metalloproteinase inducer expression during aging in rats and mice

In WT mice, cardiac EMMPRIN protein expression continuously increased with age (*Fig. 1A* and *1B*) and was associated with cardiac dysfunction (*Fig. 2*). Aging was also associated with continuous increase in EMMPRIN protein expression in rat myocardium (*Fig. 1C* and *1D*), especially at 28 and 32 months of age where a LV dysfunction and heart failure has been reported at these advanced ages (10). Fluorescent immunolabeling revealed a distinct EMMPRIN staining pattern around the sarcolemmal-interstitial interface in both mice and rats cardiomyocytes (*Fig. 1A* and *1D*, respectively), confirming that EMMPRIN is localized along the membrane surface of cardiomyocytes which is consistent with the known localization of this glycoprotein. The immunolabeling was particularly strong at the level of intercalated disc, visible at higher magnification at all ages (*Fig. 1E*), unlike the homogeneous pattern of staining that was observed in myocytes in culture (14).

In KO mice, no immunostaining could be observed in the myocardium (*Fig. 1A*) and only weak background fluorescence could be quantified (*Fig. 1B*).

Left ventricular chamber function and geometry in wild-type and extracellular matrix metalloproteinase inducer knock-out mice

Echocardiography measurements in WT mice showed an enlargement of the LV chamber only in the 24 month old when compared to both 3 and 12 month old WT mice, as indicated by the increased LV internal diameter in diastole and the increased LV end-diastolic volume, although fractional shortening and LV ejection fraction were unchanged (*Fig. 2*). In addition, LV posterior wall as well as septum thicknesses were increased at 24 months of age (0.808 ± 0.008 and 0.725 ± 0.025 mm respectively vs. 0.725 ± 0.017 and 0.583 ± 0.017 mm respectively in 3 month old mice; both $P < 0.05$).

While 3 month old EMMPRIN KO mice had similar LV dimensions and function as the 3 month old WT mice (*Fig. 2*), the 12 month old EMMPRIN KO mice already exhibited the reduced LV fractional shortening, reduced ejection fraction and higher LV end-systolic volume observed in the 24 month old WT mice (*Fig. 2*). In addition, the LV internal diameter in diastole, as well as the LV end-diastolic volume, was also greater in the 12 month old KO mice demonstrating enlarged LV chamber. This was associated with LV hypertrophy characterized by increased LV mass/body weight index (*Fig. 2B*). Thus, persistent myocardial EMMPRIN deficiency caused LV dilation, pump dysfunction, and hypertrophy in middle-aged mice.

Interestingly the differences in cardiac function and in LV dimensions or thicknesses between the WT and the EMMPRIN KO mice at 12 months of age could no longer be observed in the aged 24 month old mice (*Fig. 2B*). These results suggest that dilated cardiopathy first characterized by increased LV dimensions and hypertrophy occurs earlier in the EMMPRIN KO mice and is associated with LV dysfunction.

Left ventricular chamber fibrosis in wild-type and extracellular matrix metalloproteinase inducer knock-out mice

Masson's Trichrome staining, used to reveal ECM accumulation, fibrosis and myocyte loss, shows an excessive interstitial (*Fig. 3A*) and perivascular (*Fig. 3B*) collagen deposition (shown in blue) in 12 and 24 month old WT hearts. These results were confirmed by Sirius red staining, illustrated in *Fig. 3C*, and quantified in *Fig. 3D*, which demonstrates progressive interstitial collagen fiber deposition in 12 and 24 month old WT mice when compared to the 3 month old mice. In contrast, in the absence of EMMPRIN, the collagen content remained constant at all ages, suggesting the absence of age-associated fibrosis in this KO model. It is interesting that in the KO mice, collagen fibers were seen around myocytes, but not in the interstitial spaces corresponding to myocyte loss (*Fig. 3A* and *3C*).

Matrix metalloproteinases, fibroblasts and uPA in wild-type and extracellular matrix metalloproteinase inducer knock-out mice

MMP quantification have shown an age-related decrease in all MMPs studied in WT mice, except for MMP-9 wherein the decrease is not significant (*Fig. 4A*). This decrease appeared to be accelerated in the myocardium of KO mice, since at 12 months of age, both collagen degrading MMPs, MMP-1 and MT1-MMP, although not MMP-2, were significantly lower in the EMMPRIN KO (*Fig. 4A* and *4B*). Quantification of fibroblasts shows an increase in 24 month old mice which is not modified in EMMPRIN KO mice (*Fig. 4C*). In addition, uPA, also shown to be regulated by EMMPRIN (15), was lower in the 12 month old KO mice compared with same age WT ($P < 0.05$; *Fig. 4D* and *4E*). Hence, the age-related decrease in the proteolytic potential of the myocardium occurs earlier in the EMMPRIN KO mice.

Alterations of adherens, tight and gap junctions in wild-type and extracellular matrix metalloproteinase inducer knock-out mice

Alterations of adherens, tight and gap junctions may impair myocyte to myocyte interaction in the heart but localization of Cx-43, ZO-1 and Pan-cadherin was unaltered in the KO mice as compared to WT, whatever the age of the animals (*Fig. 5*).

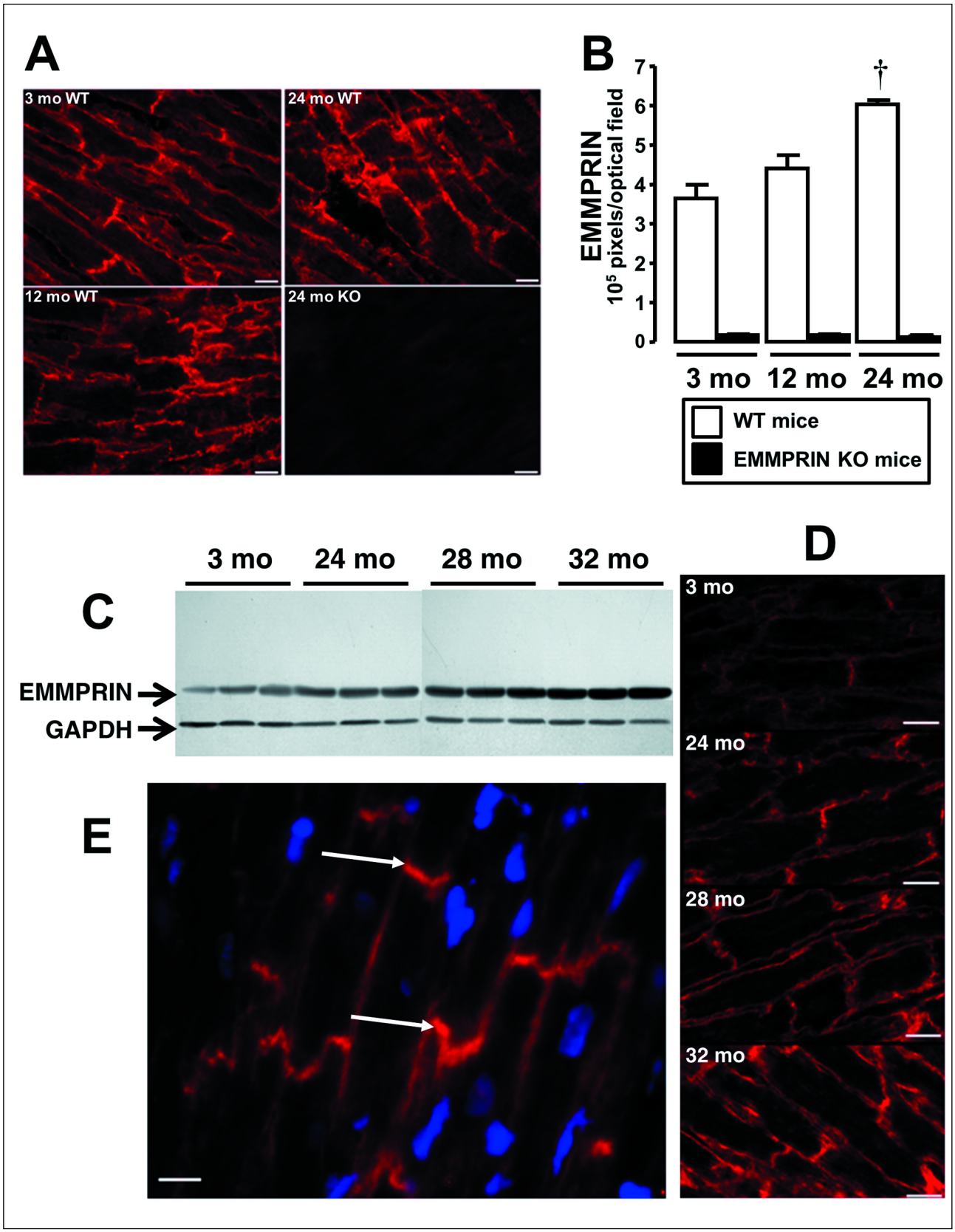

Fig. 1. EMMPRIN protein expression during aging in rodents; A: representative immunolabeling of EMMPRIN (Bar:10 µm) in mice; B: quantification of EMMPRIN in left ventricle from 3, 12 and 24 month old (mo) wild-type (WT) and EMMPRIN knock-out (KO) mice indicating an age-associated increase in EMMPRIN in WT mice and the lack of EMMPRIN in KO mice at all ages. †P < 0.05 vs. 3 month old (mo) WT mice. All P are significant between WT and KO mice; C: representative western blotting expression of EMMPRIN in rats; D: immunolabeling of EMMPRIN (Bar: 20 µm) in myocardium from 3, 24, 28 and 32 month old rats, showing that EMMPRIN increased with age. E: Higher magnification of EMMPRIN labeling in 3 month old heart section (Bar: 10 µm) showing a main localization at intercalated disk (arrows) but also on all the sarcolemna.

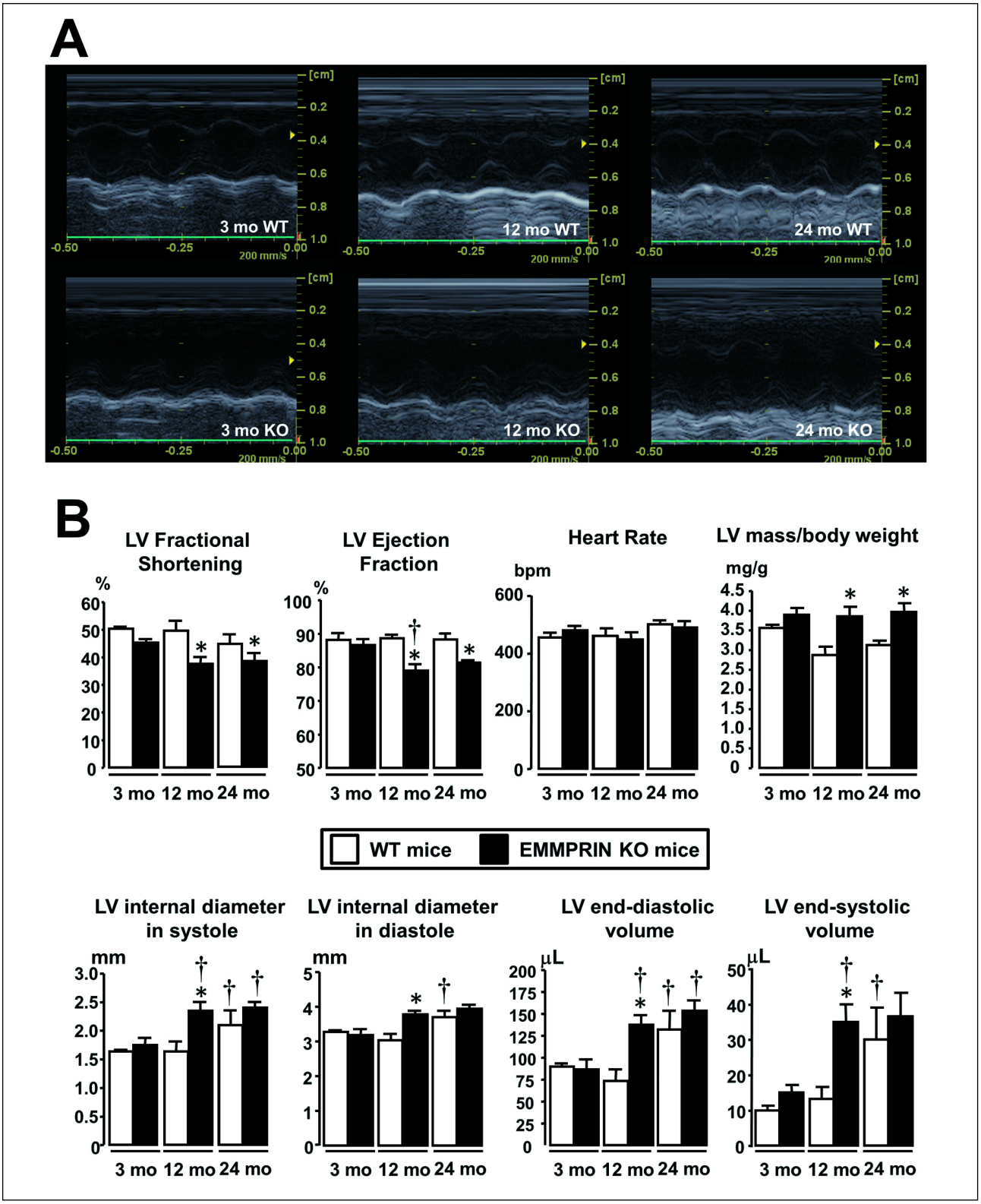

Fig. 2. Cardiac function measured by echocardiography during aging and EMMPRIN deficiency in mice. A: representative M-mode echocardiography in 3, 12 and 24 month old (mo) WT and 24 month old EMMPRIN KO, showing a significant left ventricular (LV) dilatation, evident in 24 month old WT mice but also in 12 and 24 month old EMMPRIN KO mice. B: echocardiographic measurements of LV volumes, function, and mass normalized by body weight in 3, 12 and 24 month old WT and EMMPRIN KO mice, demonstrating an increase in LV internal diameters and LV hypertrophy associated with an impairment of LV fractional shortening and ejection fraction at 12 months of age in EMMPRIN KO mice. The LV mass and the percent shortening fraction was calculated from M-mode measurements as follows: LV mass = 1.055 [(end-diastolic interventricular septum thickness + LV end-diastolic posterior wall thickness + LV end-diastolic diameter)^3 - (LV end-diastolic diameter)^3] where 1.055 is the specific gravity of the myocardium; % Fractional shortening = 100 [(LV end-diastolic diameter - LV end-systolic diameter) / LV end-diastolic diameter], *P < 0.05 vs. WT age-matched mice, †P < 0.05 vs. pathology-matched 3 month old mice.

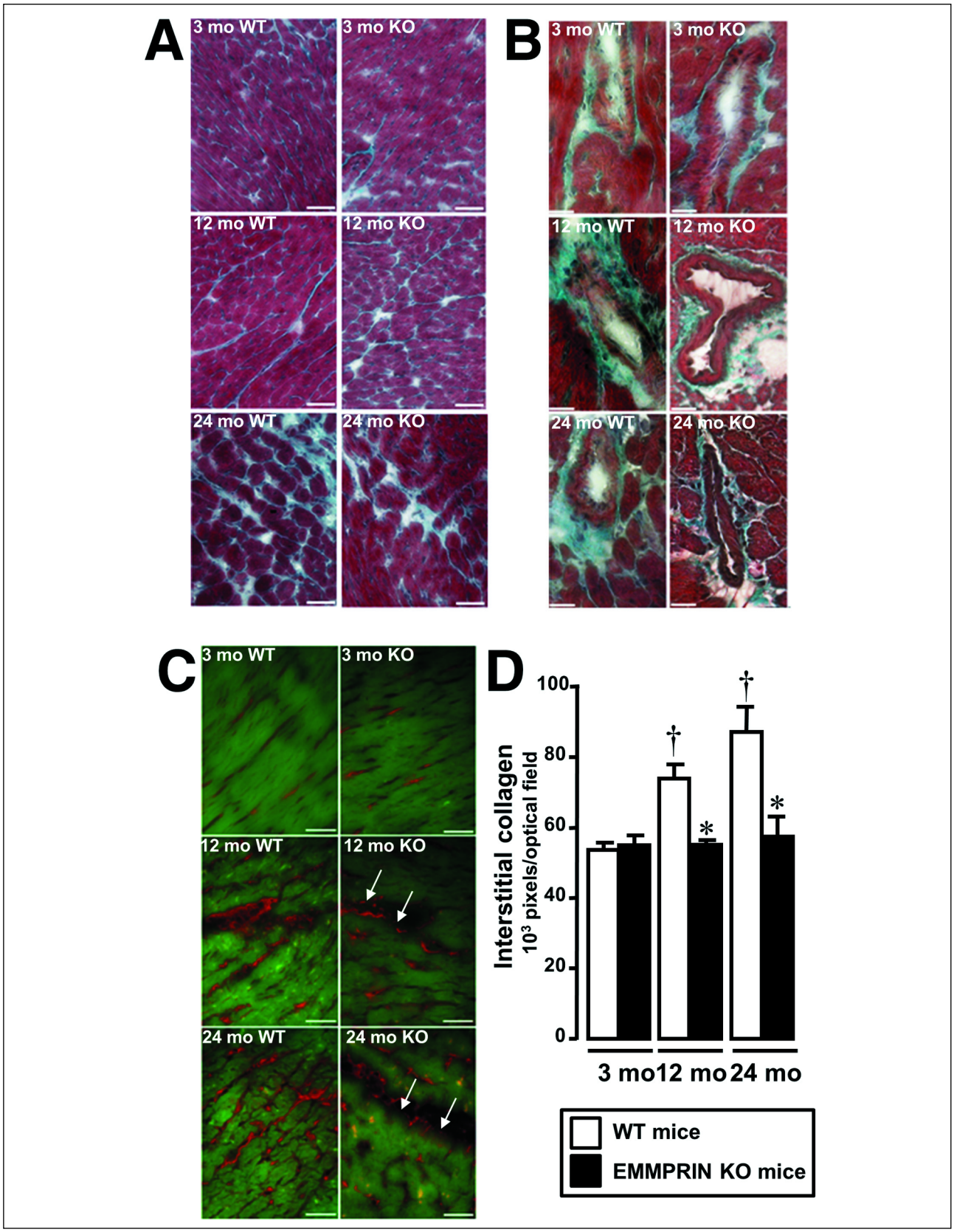

Fig. 3. Cardiac collagen distribution during aging and EMMPRIN deficiency in mice. A and B: representative micrographs of LV sections stained with Masson's trichrome showing, in blue, interstitial (Bar: 10 μm) and perivascular (Bar: 20 μm) fibrosis, respectively. C: representative micrographs of LV sections stained with picrosirius red showing, in red, fibrillar collagen network (Bar: 10 μm) surrounding cardiomyocytes (green due to autofluorescence), respectively in 3, 12 and 24 month old (mo) WT and 24 month old EMMPRIN KO mice. Disruption of perimysial collagen fibers was present in both 12 and 24 month old EMMPRIN KO mice (arrows). D: quantification of interstitial collagen in picrosirius red stained sections by image analysis in all experimental groups showing no age-associated collagen deposition in EMMPRIN KO mice. *$P < 0.05$ vs. age-matched WT mice; †$P < 0.05$ vs. 3 month old pathology-matched mice.

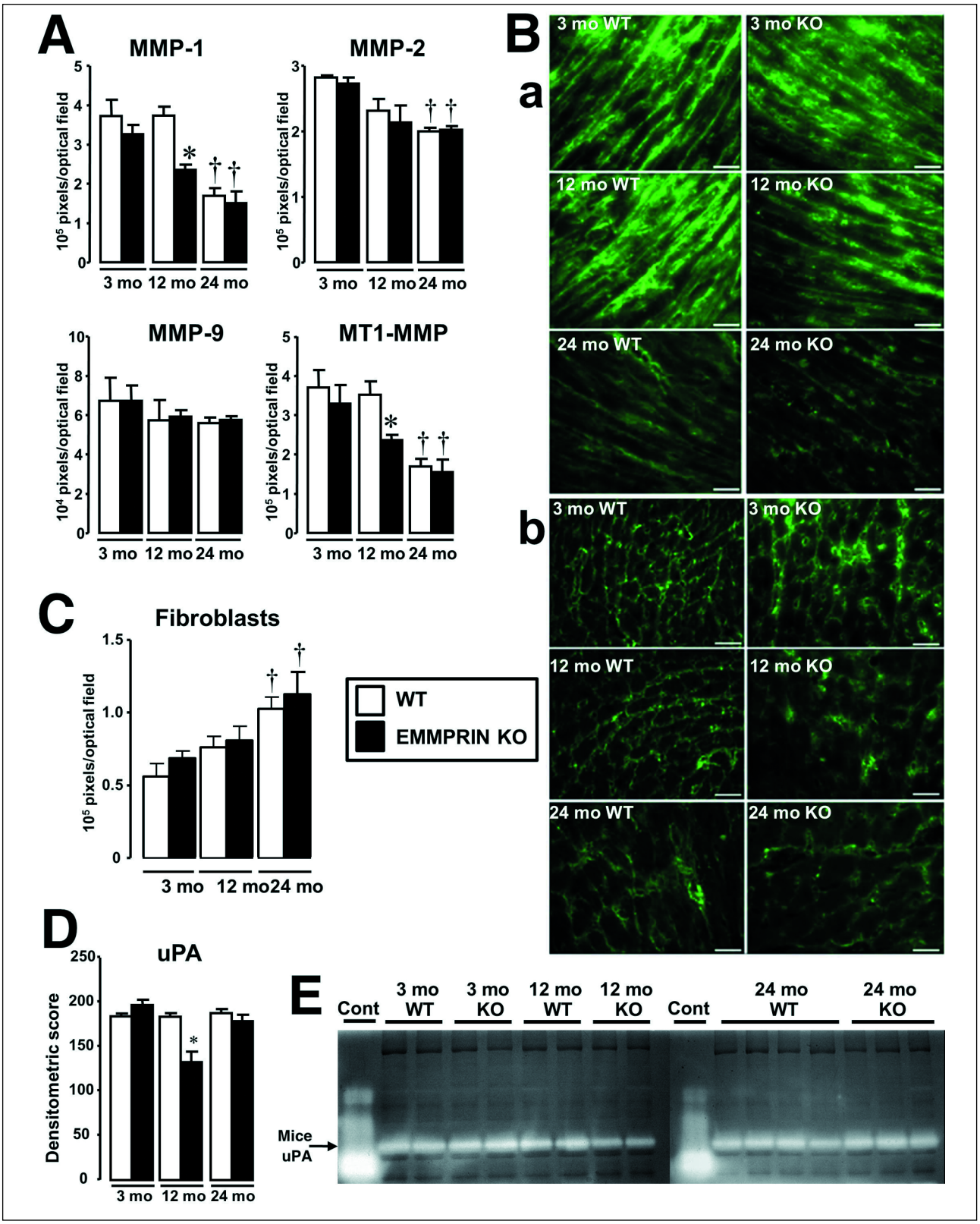

Fig. 4. MMPs, fibroblasts and uPA quantification during aging and EMMPRIN deficiency in mice. A: quantification of MMP-1, MMP-2, MMP-9 and MT1-MMP in immunostained LV sections from 3, 12 and 24 month old (mo) WT and EMMPRIN KO mice showing unchanged MMP-2 and MMP-9 levels in KO mice but a decrease in MMP-1 and MT1-MMP as soon as 12 months of age. *P < 0.05 vs. age-matched WT mice; †P < 0.05 vs. 3 month old pathology-matched mice. B: representative micrographs of LV immunofluorescent staining of MMP-1 (a) and MT1-MMP (b) in 3, 12 and 24 month old WT and EMMPRIN KO mice illustrating their decrease in 12 month old EMMPRIN deficient mice. Bar: 50 µm. C: quantification of fibroblasts in immunostained LV sections from 3, 12 and 24 month old WT and EMMPRIN KO mice. D: densitometric quantification of uPA activity in 3, 12 and 24 month old WT and EMMPRIN KO mice showing decreased uPA activity in 12 month old KO mice, *P < 0.05 vs. age-matched WT mice. E: representative micrographs of gels of casein zymography; conditioned medium of human fibrosarcoma HT 1080 cells was used as positive control (Cont).

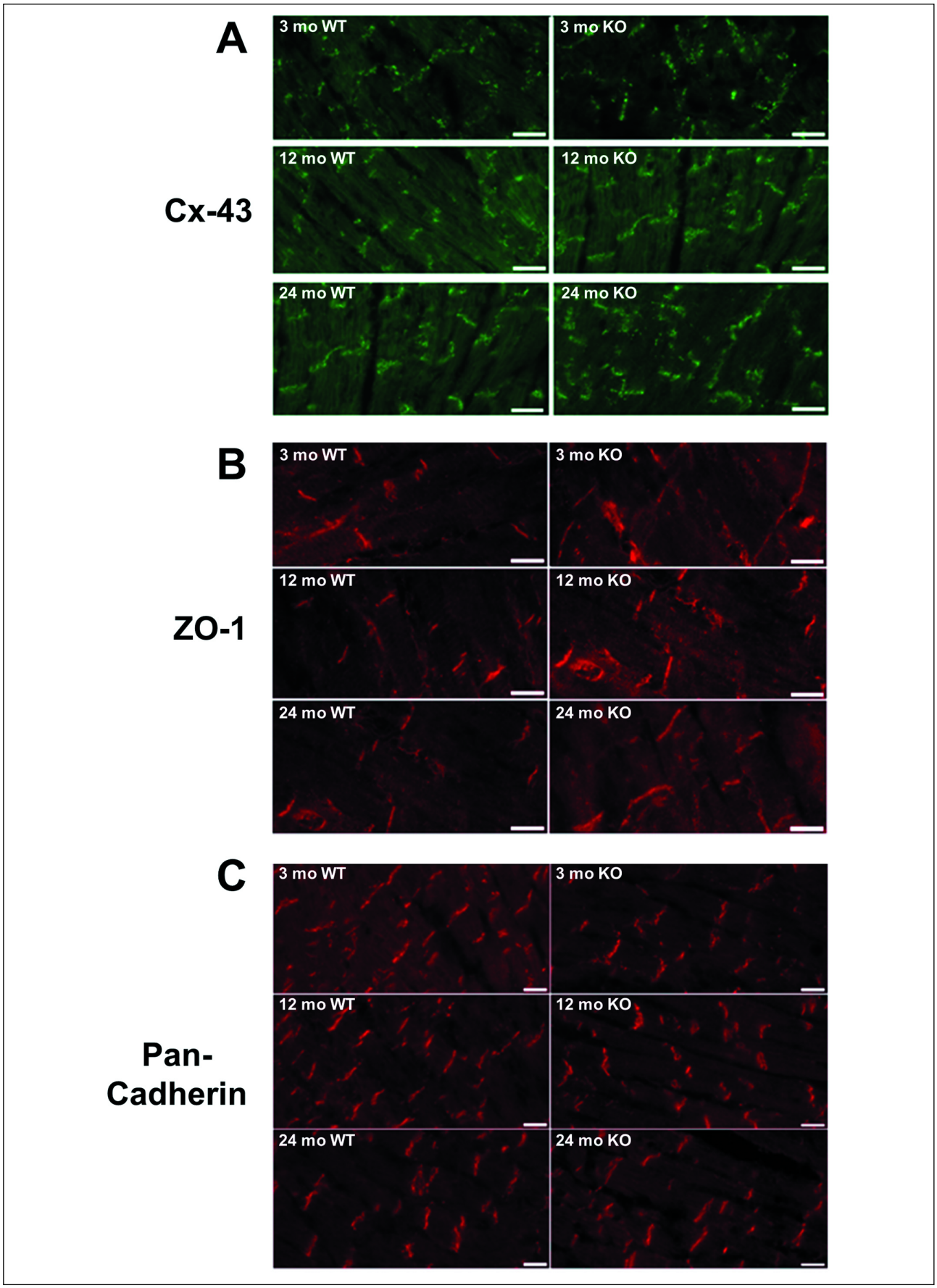

Fig. 5. Immunofluorescent staining of gap (A: Cx-43), tight (B: ZO-1) and adherens (C: Pan-Cadherin) junctions during aging and EMMPRIN deficiency in mice. The localization of Cx-43, ZO-1 and Pan-cadherin was unaltered in the EMMPRIN knock-out (KO) as compared to wild-type (WT) mice of the same age at 3, 12 and 24 months of age. Bar: 20 μm.

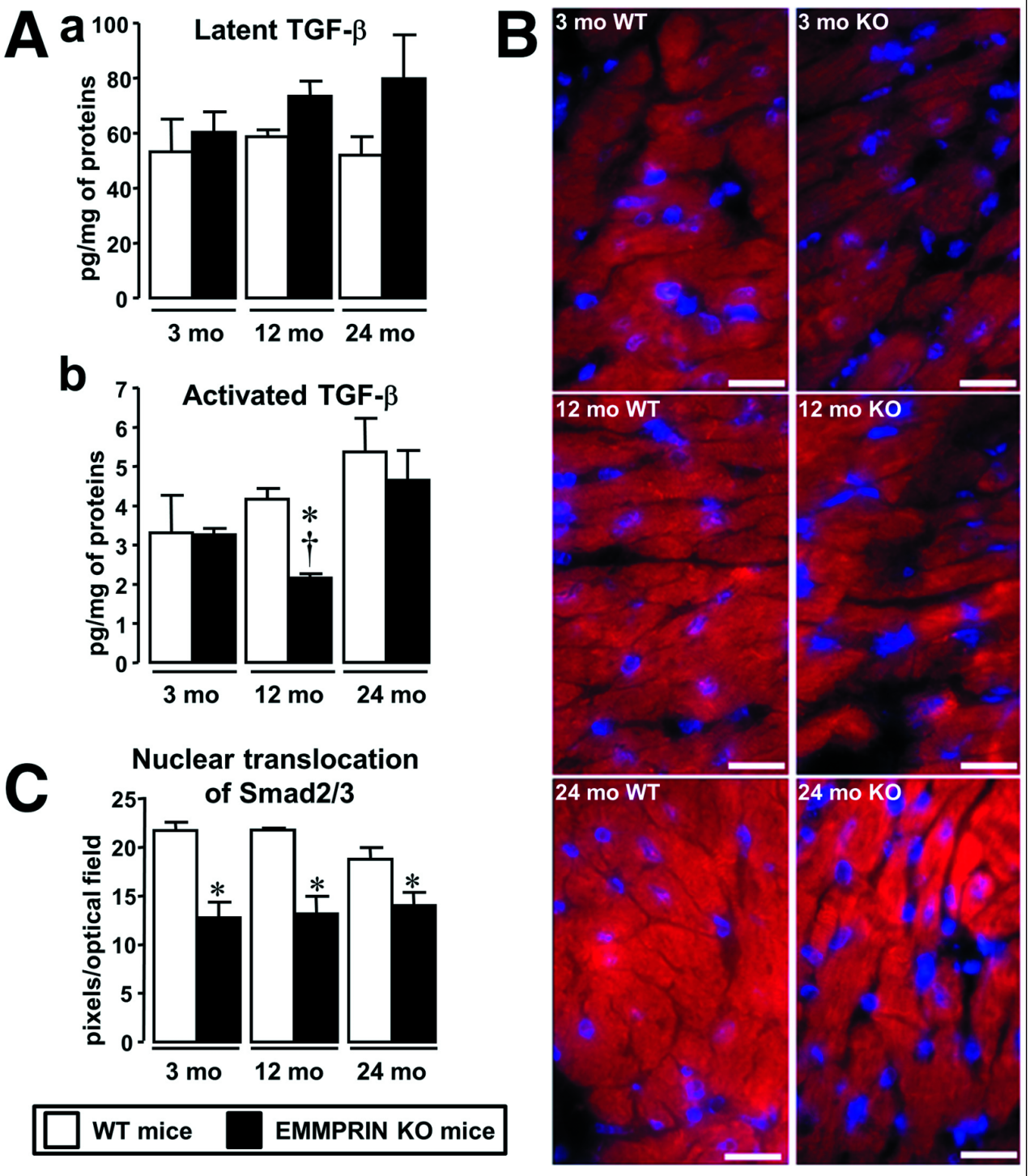

Fig. 6. Cardiac transforming growth factor-β (TGF-β) content and nuclear translocation of smad2/3 during aging and EMMPRIN deficiency in mice. A: quantification of concentrations of latent (a) and activated (b) TGF-β, respectively in left ventricle from 3, 12 and 24 month old (mo) WT and 24 month old EMMPRIN KO mice, indicating that activated TGF-β was decreased in 12 month old EMMPRIN KO mice. *$P < 0.05$ vs. age-matched WT mice; †$P < 0.05$ vs. 3 month old pathology-matched mice. B: representative micrographs of smad2/3 nuclear translocation, detected by a purple staining, and resulting from the co-localization of smad2/3 immunolabeling in red and nuclear counterstaining with DAPI in blue in 3, 12 and 24 month old WT and EMMPRIN KO mice. Bar: 10 μm. C: quantification of nuclear translocation of smad2/3, showing reduction of smad2/3 nuclear translocation at all ages in EMMPRIN KO mice as compared to age-matched WT mice. *$P < 0.05$ vs. age-matched WT mice.

Transforming growth factor-β activation and smad2/3 nuclear translocation

Because TGF-β is known to induce synthesis of collagen *via* the activation of smad signaling, cardiac latent and activated TGF-β content as well as smad2/3 activation were quantified in WT and KO mice (*Fig. 6*). While aging was associated with cardiac fibrosis, neither latent (*Fig. 6A*) nor activated (*Fig. 6B*) TGF-β were significantly increased in 12 and 24 month old WT mice and smad 2/3 nuclear translocation was similar at all ages (*Fig. 6C* and *6D*). In contrast, in KO mice, smad2/3 nuclear translocation was much reduced at 3, 12 as well as 24 month old compared to same age WT mice (*Fig. 6C* and *6D*). At 12 but not at 24 months of age, this impairment of smad2/3 translocation was associated with a decrease in activated TGF-β levels with no significant increase in latent TGF-β (*Fig. 6*). Hence, TGF-β activation was attenuated in the 12 month old myocardium of EMMPRIN KO mice, as was also shown above for the MT1-MMP and uPA, enzymes previously shown to be able to activate TGF-β.

DISCUSSION

The results described in the present study show that selective disruption of the EMMPRIN gene leads to impaired cardiac function in middle aged mice, presenting a phenotype with dilated cardiopathy characterized by LV dilation and hypertrophy and associated with pump dysfunction. This phenotype appears to be associated with a reduction in cardiac fibrosis which is generally observed during normal aging, underscoring the importance of the fibrotic process in the protection and preservation of the cardiac function of the aging animals. The lower expression of MT1-MMP and uPA, as well as the repressed activation of TGF-β, a major fibrotic cytokine known to stimulate collagen synthesis, may be responsible for the decreased collagen deposition in the absence of EMMPRIN.

Cardiac ECM remodeling during aging, concomitant to myocyte loss, collagen deposition and age-related cardiac fibrosis has been constantly reported in humans as in animals (16, 17). Such active fibrotic remodeling, which may be initially protective, eventually results in the activation of matrix-degrading pathways, leading to the development of ventricular dilation and may induce systolic failure at advanced ages (10, 11, 18). Indeed, LV dilatation, evidenced by the increased in both LV internal diameters and volumes in systole and diastole, was also observed in the aged 24 month old WT mice in this study, as in others previously (19, 20).

EMMPRIN, mainly known for its ability to induce the expression of MMPs in tumor invasion and metastasis, has recently been proposed as an upstream signaling pathway that can play a role in adverse remodeling within the myocardium (4, 21). Its upregulation in multiple cell types appears to be critical in the transcriptional regulation of MMPs. An age-associated increase in EMMPRIN was observed in the present study in both rat and mouse hearts, which may be the result from an increase in the reactive oxygen species (14) and/or inflammatory cytokines (21), known as EMMPRIN inductors.

Unlike WT mice, the examination of EMMPRIN deficient mice did not reveal any detected cardiac fibrosis. Indeed, while interstitial collagen content WT mice was shown to increase with age, it remained fairly constant in the 3, 12 and 24 month old EMMPRIN KO mice. Similar results were recently reported in unilateral ureteral obstruction model where renal fibrosis was reduced in EMMPRIN KO mice (22). The lack of detected fibrosis in EMMPRIN KO mice is unlikely to be due to fibroblast content which remained constant when compared to WT mice of the same age, suggesting therefore that an impaired synthesis and/or secretion of collagen by fibroblasts may be a more plausible cause for inhibiting fibrosis in this KO model.

In view of this apparent role of EMMPRIN in fibrosis, it is tempting to hypothesize that in the absence of EMMPRIN, the age-related myocyte loss would not be replaced by a reparative fibrosis, disrupting the integrity of the matrix around the remaining myocytes and subsequently impairing coordinated contraction. Interestingly, whatever benefits the fibrotic effect endowed the WT middle-aged mice, it was no longer advantageous at the old ages, as the both WT and EMMPRIN KO mice presented similar cardiomyopathy when the mice reached 24 months. Moreover EMMPRIN persistent myocardial expression has been shown to cause cardiomyopathy in middle aged mice, with increased fibrosis associated with increased levels of MT1-MMP and active MMP-2 (9). Considering both this study and ours, it appears that elevation or suppression of EMMPRIN may have an opposite effect on fibrosis but results in the same type phenotype i.e. a dilated cardiomyopathy, confirming the central role played by cardiac extracellular matrix, and especially collagen content in cardiac function.

Different studies have previously reported that dilated cardiopathy may also result from the abnormal expression and/or localization of proteins involved in cell-cell communication (23). While we previously reported that EMMPRIN regulates tight junctions in corneal epithelium (24), our present results in heart failed to show alterations in either adherens, tight and gap junctions, in EMMPRIN KO mice, excluding a role for EMMPRIN in the regulation of myocytes cell-cell interaction as the cause of LV dilation observed in the EMMPRIN KO hearts.

Matrix degrading matrix proteinases, including MMPs and some serine proteinases, can have a direct effect on matrix turnover by degrading its constituents. A dysregulation of MMPs, which initiate and execute proteolytic degradation of the fibrillar collagen types I and III, has been described in heart failure and myocardial infarction (4, 5) but also in atherosclerotic plaque (25). In heart, a cause-effect relation between matrix degrading matrix proteinases and an aberrant ECM remodeling which leads to cardiopathy has been well described using transgenic models (4, 26, 27). Intuitively, one would expect that EMMPRIN deficiency will result in more fibrosis in view of its role in MMPs production and hence in matrix degradation. However, while the cardiac tissues of the 12 month old EMMPRIN KO mice expressed lower levels of MMP-1 and MT1-MMP and uPA, but not of MMP-2 and MMP-9, this decrease in proteases was associated with marked reduction of fibrosis. Similarly, in atherosclerotic plaque, a decrease in MMP activities is also associated with a decrease in collagen content after treatment with β1 blocker (25). However, the regulation of the MMP activation in myocardium is complex and not completely understood. For example, numerous studies reported that MMP-9 was predominantly produced by leukocytes and macrophages in different cardiac diseases, but a recent study reported that MMP-9 also originates from cardiomyocytes and may serve as a reservoir of active MMP-9 (28). Total MMP-9 is unchanged in our study during cardiac aging as well as in EMMPRIN-KO mice but the distribution of such MMP-9 production from inflammatory cells and/or from cardiomyocytes is presently unknown.

The observed reduction of fibrosis in EMMPRIN KO mice also concords with several studies implicating EMMPRIN in the process of fibrosis of different organs such as kidney and liver (22, 29) and underlines the complex role of MMPs in matrix turnover as an increased expression of several MMPs has already been shown to be associated with increased fibrosis (30). In particular, less cardiac fibrosis was observed in uPA KO mice than heterozygote mice (31). While myocardial overexpression of

MMP-1 was associated with an increased collagen content in the 6 month old animals, the authors described a loss of cardiac interstitial collagen at 12 months of age which coincided with systolic and diastolic dysfunction (27). In another study, the overexpression of MT1-MMP induced cardiac collagen deposition during pressure overload (5) as well as in the infarcted scar after myocardial infarction (4) compared to WT and heterozygotes (4).

The implication of TGF-β in cardiac myopathy has also been largely demonstrated, and suppressing smad signaling by neutralizing antibodies or smad3 deletion was shown to block cardiac fibrosis *in vitro* and *in vivo* (32, 33). Several proteinases have been shown to be able to activate latent TGF-β (34) and can therefore promote fibrosis through smad activation. In the EMMPRIN KO mice, both uPA and MT1-MMP, proteinases previously shown to be potential TGF-β activators, are lower, consistent with the decrease in both activated TGF-β and smad2/3 nuclear translocation which may explain, at least in part, the decrease in collagen deposition in this EMMPRIN KO model. These results are consistent with our previous publications where in both a corneal wound healing model (35) as well as in a muscle model system (36). TGF-β signaling and fibrotic effects were increased by the addition of recombinant EMMPRIN and inhibited by EMMPRIN silencing. It is noteworthy that the increased fibrotic process observed during normal aging in the WT mice was not associated with a detectable increase in the activation of TGF-β, underlining the complex interplay between EMMPRIN, proteinases and TGF-β in the development of fibrosis. Additional experiments would be required to clarify the precise role of EMMPRIN on TGF-β signaling, as well as its role on other pathways involved in the pathogenesis of cardiac fibrosis in the senescent heart, such as angiotensin II, reactive oxygen species, beta-adrenergic signaling, C-type natriuretic peptide or endothelin-1 signaling to explain the altered mechanism(s) of fibrosis in the KO mice. Indeed, it has been previously proposed that other cytokines or agonists capable of activating MAP kinases, such as PDGF in liver injury, are also able to activate collagen transcription through smad2/3 nuclear translocation (37) and potential interactions between EMMPRIN and these different pathways are presently unknown.

In conclusion, we demonstrate in this study that EMMPRIN gene silencing is associated with an aberrant ECM remodeling, characterized by a striking reduction in age-associated fibrosis and results in dilated cardiomyopathy and impairment of ejection fraction. This phenotype closely resembles that observed during cardiac EMMPRIN overexpression (4) suggesting that the fine regulation of EMMPRIN is essential for the coordinated ECM remodeling during aging.

Abbreviations: Cnx43 : connexin 43; ECM : extracellular matrix; ELISA : enzyme-linked immunosorbent assay; EMMPRIN : extracellular matrix metalloproteinase inducer; KO: knock-out; LV: left ventricular; MMP: matrix metalloproteinase; MT1-MMP: membrane type-1-matrix metalloproteinase; TGF-β: transforming growth factor-β; uPA: urokinase plasminogen activator; WT: wild type; ZO-1: zonula occludens 1.

Acknowledgements: Authors E. Gabison and B. Vallee equally contributed to the work.

Conflict of interests: None declared.

REFERENCES

1. Rozenberg S, Tavernier B, Riou B, *et al.* Severe impairment of ventricular compliance accounts for advanced age-associated hemodynamic dysfunction in rats. *Exp Gerontol* 2006; 41: 289-295.
2. Fukuta H, Little WC. Contribution of systolic and diastolic abnormalities to heart failure with a normal and a reduced ejection fraction. *Prog Cardiovasc Dis* 2007; 49: 229-240.
3. Fedak PW, Altamentova SM, Weisel RD, *et al.* Matrix remodeling in experimental and human heart failure: a possible regulatory role for TIMP-3. *Am J Physiol Heart Circ Physiol* 2003; 284: H626-H634.
4. Zavadzkas JA, Mukherjee R, Rivers WT, *et al.* Direct regulation of membrane type 1 matrix metalloproteinase following myocardial infarction causes changes in survival, cardiac function, and remodeling. *Am J Physiol Heart Circ Physiol* 2011; 301: H1656-H1666.
5. Zile MR, Baicu CF, Stroud RE, *et al.* Pressure overload-dependent membrane type 1-matrix metalloproteinase induction: relationship to LV remodeling and fibrosis. *Am J Physiol Heart Circ Physiol* 2012; 302: H1429-H1437.
6. Nagase H, Visse R, Murphy G. Structure and function of matrix metalloproteinases and TIMPs. *Cardiovasc Res* 2006; 69: 562-573.
7. Iacono KT, Brown AL, Greene MI, Saouaf SJ. CD147 immunoglobulin superfamily receptor function and role in pathology. *Exp Mol Pathol* 2007; 83: 283-295.
8. Biswas C, Zhang Y, DeCastro R, *et al.* The human tumor cell-derived collagenase stimulatory factor (renamed EMMPRIN) is a member of the immunoglobulin superfamily. *Cancer Res* 1995; 55: 434-439.
9. Zavadzkas JA, Plyler RA, Bouges S, *et al.* Cardiac-restricted overexpression of extracellular matrix metalloproteinase inducer causes myocardial remodeling and dysfunction in aging mice. *Am J Physiol Heart Circ Physiol* 2008; 295: H1394-H1402.
10. Besse S, Boucher F, Linguet G, *et al.* Intramyocardial protein therapy with vascular endothelial growth factor (VEGF-165) induces functional angiogenesis in rat senescent myocardium. *J Physiol Pharmacol* 2010; 61: 651-661.
11. Pacher P, Mabley JG, Liaudet L, *et al.* Left ventricular pressure-volume relationship in a rat model of advanced aging-associated heart failure. *Am J Physiol Heart Circ Physiol* 2004; 287: H2132-H2137.
12. Igakura T, Kadomatsu K, Taguchi O, *et al.* Roles of basigin, a member of the immunoglobulin superfamily, in behavior as to an irritating odor, lymphocyte response, and blood-brain barrier. *Biochem Biophys Res Commun* 1996; 224: 33-36.
13. Igakura T, Kadomatsu K, Kaname T, *et al.* A null mutation in basigin, an immunoglobulin superfamily member, indicates its important roles in peri-implantation development and spermatogenesis. *Dev Biol* 1998; 194: 152-165.
14. Siwik DA, Kuster GM, Brahmbhatt JV, *et al.* EMMPRIN mediates beta-adrenergic receptor-stimulated matrix metalloproteinase activity in cardiac myocytes. *J Mol Cell Cardiol* 2008; 44: 210-217.
15. Quemener C, Gabison EE, Naimi B, *et al.* Extracellular matrix metalloproteinase inducer up-regulates the urokinase-type plasminogen activator system promoting tumor cell invasion. *Cancer Res* 2007; 67: 9-15.
16. Chen W, Frangogiannis NG. The role of inflammatory and fibrogenic pathways in heart failure associated with aging. *Heart Fail Rev* 2010; 15: 415-422.
17. Besse S, Robert V, Assayag P, Delcayre C, Swynghedauw B. Nonsynchronous changes in myocardial collagen mRNA and protein during aging: effect of DOCA-salt hypertension. *Am J Physiol* 1994; 267: H2237-H2244.
18. Yang B, Larson DF, Watson R. Age-related left ventricular function in the mouse: analysis based on in vivo pressure-volume relationships. *Am J Physiol* 1999; 277: H1906-H1913.

19. Boyle AJ, Shih H, Hwang J, *et al.* Cardiomyopathy of aging in the mammalian heart is characterized by myocardial hypertrophy, fibrosis and a predisposition towards cardiomyocyte apoptosis and autophagy. *Exp Gerontol* 2011; 46: 549-559.
20. Derumeaux G, Ichinose F, Raher MJ, *et al.* Myocardial alterations in senescent mice and effect of exercise training: a strain rate imaging study. *Circ Cardiovasc Imaging* 2008; 1: 227-234.
21. Schmidt R, Bultmann A, Ungerer M, *et al.* Extracellular matrix metalloproteinase inducer regulates matrix metalloproteinase activity in cardiovascular cells: implications in acute myocardial infarction. *Circulation* 2006; 113: 834-841.
22. Kato N, Kosugi T, Sato W, *et al.* Basigin/CD147 promotes renal fibrosis after unilateral ureteral obstruction. *Am J Pathol* 2011; 178: 572-579.
23. Sheikh F, Ross RS, Chen J. Cell-cell connection to cardiac disease. *Trends Cardiovasc Med* 2009; 19: 182-190.
24. Huet E, Vallee B, Delbe J, *et al.* EMMPRIN modulates epithelial barrier function through a MMP-mediated occludin cleavage: implications in dry eye disease. *Am J Pathol* 2011; 179: 1278-1286.
25. Pyka-Fosciak G, Jawien J, Gajda M, Jasek E, Litwin JA. Effect of nebivolol treatment on atherosclerotic plaque components in apoE-knockout mice. *J Physiol Pharmacol* 2013; 64: 745-750.
26. Li YY, McTiernan CF, Feldman AM. Interplay of matrix metalloproteinases, tissue inhibitors of metalloproteinases and their regulators in cardiac matrix remodeling. *Cardiovasc Res* 2000; 46: 214-224.
27. Kim HE, Dalal SS, Young E, Legato MJ, Weisfeldt ML, D'Armiento J. Disruption of the myocardial extracellular matrix leads to cardiac dysfunction. *J Clin Invest* 2000; 106: 857-866.
28. Kiczak L, Tomaszek A, Bania J, *et al.* Matrix metalloproteinase 9/neutrophil gelatinase associated lipocalin/tissue inhibitor of metalloproteinasess type 1 complexes are localized within cardiomyocytes and serve as a reservoir of active metalloproteinase in porcine female myocardium. *J Physiol Pharmacol* 2014; 65: 365-375.
29. Guillot S, Delaval P, Brinchault G, *et al*. Increased extracellular matrix metalloproteinase inducer (EMMPRIN) expression in pulmonary fibrosis. *Exp Lung Res* 2006; 32: 81-97.
30. Radisky DC, Przybylo JA. Matrix metalloproteinase-induced fibrosis and malignancy in breast and lung. *Proc Am Thorac Soc* 2008; 5: 316-322.
31. Stempien-Otero A, Plawman A, Meznarich J, Dyamenahalli T, Otsuka G, Dichek DA. Mechanisms of cardiac fibrosis induced by urokinase plasminogen activator. *J Biol Chem* 2006; 281: 15345-15351.
32. Kuwahara F, Kai H, Tokuda K, *et al.* Transforming growth factor-beta function blocking prevents myocardial fibrosis and diastolic dysfunction in pressure-overloaded rats. *Circulation* 2002; 106: 130-135.
33. Divakaran V, Adrogue J, Ishiyama M, *et al.* Adaptive and maladptive effects of SMAD3 signaling in the adult heart after hemodynamic pressure overloading. *Circ Heart Fail* 2009; 2: 633-642.
34. Jenkins G. The role of proteases in transforming growth factor-beta activation. *Int J Biochem Cell Biol* 2008; 40: 1068-1078.
35. Huet E, Vallee B, Szul D, *et al.* Extracellular matrix metalloproteinase inducer/CD147 promotes myofibroblast differentiation by inducing alpha-smooth muscle actin expression and collagen gel contraction: implications in tissue remodeling. *FASEB J* 2008; 22: 1144-1154.
36. Attia M, Huet E, Delbe J, Ledoux D, Menashi S, Martelly I. Extracellular matrix metalloproteinase inducer (EMMPRIN/CD147) as a novel regulator of myogenic cell differentiation. *J Cell Physiol* 2011; 226: 141-149.
37. Matsuzaki K. Smad phosphoisoform signals in acute and chronic liver injury: similarities and differences between epithelial and mesenchymal cells. *Cell Tissue Res* 2012; 347: 225-243.

Received: April 10, 2014
Accepted: March 6, 2015

Author's address: Dr. Sophie Besse, Unite de Biologie Integrative des Adaptions a l'Exercise, INSERM U902, Universite d'Evry-Val d'Essonne, Boulevard F. Mitterand, 91025 Evry cedex, France.
E-mail: Sophie.Besse@parisdescartes.fr